



ISSN: 0067-2904

## Investigating the Annual Cross-Correlation between HPF, OWF and BUF Ionospheric Parameters over Middle East Region

Aula A. Ezzat\*<sup>1,2</sup>, Khalid A. Hadi<sup>2</sup>

<sup>1</sup>Ministry of Science and Technology, Directorate of Space technology and Communication, Baghdad, Iraq

<sup>2</sup>Department of Astronomy and Space, College of Science, University of Baghdad, Baghdad, Iraq

Received: 5/10/2023

Accepted: 10/5/2024

Published: 15/11/2024

### Abstract

In this work various correlation methods were employed to investigate the annual cross-correlation patterns among three different ionospheric parameters: Optimum Working Frequency (OWF), Highest Probable Frequency (HPF), and Best Usable Frequency (BUF). The annual predicted dataset for these parameters were generated using VOCAP and ASASPS models based on the monthly Sunspot Numbers (SSN) during two years of solar cycle 24, minimum 2009 and maximum 2014. The investigation was conducted for Thirty-two different transmitter/receiver stations distributed over Middle East. The locations were selected based on the geodesic parameters which were calculated for different path lengths (500, 1000, 1500, and 2000) km and bearings (N, NE, E, SE, S, SW, W, NW) using a Matlab program that was designed and implemented for this purpose. Depending on the investigation results of the cross-correlation, a third order polynomial equation provides a better representation of the correlation between the tested parameters. Also, the annual values of the HPF, OWF, and BUF parameters were predicted using the proposed mathematical correlation equations. These equations were confirmed by comparing their results with the observed datasets for the studied years. Several statistical methods were used to validate the presented data, all of which gave good results for all tested cases. Also, contour plot diagrams were used to visually illustrate the annual average distribution pattern of the tested ionospheric parameters for all geodetic factors for the minimum and maximum years of Solar Cycle 24.

**Keywords:** HF Communication, Ionospheric Parameters, HPF, OWF, BUF, Annual Cross-correlation

التحقق من طبيعة الارتباط التبادلي السنوي بين معلمات HPF و OWF و BUF فوق منطقة الشرق الأوسط

علاء عزت\*<sup>1,2</sup> خالد عبد الكريم هادي<sup>2</sup>

<sup>1</sup>وزارة العلوم والتكنولوجيا ، دائرة تكنولوجيا الفضاء والاتصالات ، بغداد ، العراق

<sup>2</sup>قسم الفلك والفضاء ، كلية العلوم ، جامعة بغداد ، بغداد ، العراق

### الخلاصة

في هذا العمل تم استخدام طرق ارتباط مختلفة لدراسة أنماط الارتباط المتبادل للمعدل السنوي بين ثلاث من معلمات الغلاف الأيوني ، و هي Optimum Working Frequency(OWF) و Highest

\*Email: [Aula1988@yahoo.com](mailto:Aula1988@yahoo.com)

البيانات Probable Frequency (HPF) و Best Usable Frequency (BUF). تم توليد مجموعة البيانات التنبؤية السنوية للمعلمات المدروسة باستخدام نماذج VOCAP و ASASPS كدالة لقيم المعدل الشهري للبقع الشمسية (SSN) خلال عامين من الدورة الشمسية 24، الدنيا 2009 والعظمى 2014. تم إجراء التحقق لاثنتين وثلاثين محطة إرسال/استقبال مختلفة موزعة فوق منطقة الشرق الأوسط، تم اختيار المواقع بناءً على المعلمات الجيوديسية التي تم تحديدها لأطوال مسارات مختلفة (500، 1000، 1500، 2000) كم و اتجاهات متعددة (N, NE, E, SE, S, SW, W, NW) باستخدام برنامج Matlab تم تصميمه وتنفيذه لهذا الغرض. واعتماداً على نتائج التحقق للارتباط المتبادل، فإن المعادلة متعددة الحدود من الدرجة الثالثة توفر أفضل تمثيل للارتباط بين المعلمات التي تم اختبارها. كما تم التنبؤ بالقيم السنوية لمعلمات HPF و OWF باستخدام معادلات الارتباط الرياضية المقترحة. و تم التحقق من صحة هذه المعادلات من خلال مقارنة نتائجها مع مجموعة البيانات المرصودة لسنوات الدراسة. تم استخدام العديد من الطرق الإحصائية للتحقق من صحة البيانات المتوقعة، والتي أعطت جميعها نتائج جيدة و لجميع الحالات التي تم اختبارها، كما تم اعتماد المخططات الكنتورية لتوضيح نمط التوزيع (السلوك) للمعدلات السنوية للمعلمات الأيونوسفيرية المختبرة لجميع العوامل الجيوديسية للسنوات الدنيا والقصى للدورة الشمسية 24.

## 1. Introduction

The Earth's ionosphere is the upper atmospheric region that has a significant concentration of charged ions and electrons, which can be sufficiently affect the propagation of radio waves [1]. At different altitudes, the rates of ionization are influenced by the structure of the atmosphere as well as the properties of the incoming solar radiation. A structure of the ionosphere layer from low to high altitudes can be divided into three main layers D, E, and F (F1 and F2) that distinguished by their electron density and temperature as shown in Figure (1) [2, 3].

The number of layers, their altitudes, and the densities of ionization undergo changes over both time and location [4], the main factors affecting the ionosphere are day-night cycles, seasons, sunspot activity, polar auroras, and the Earth's magnetic field. The frequency range that can reflected back to Earth by the ionosphere is a high-frequency radio band (HF-band) that may vary between 2 and 30 MHz [5, 6]. There are many typical applications of HF radio waves such as shortwave international and regional broadcasting, long-distance communications, aviation, and maritime mobile communications [7].

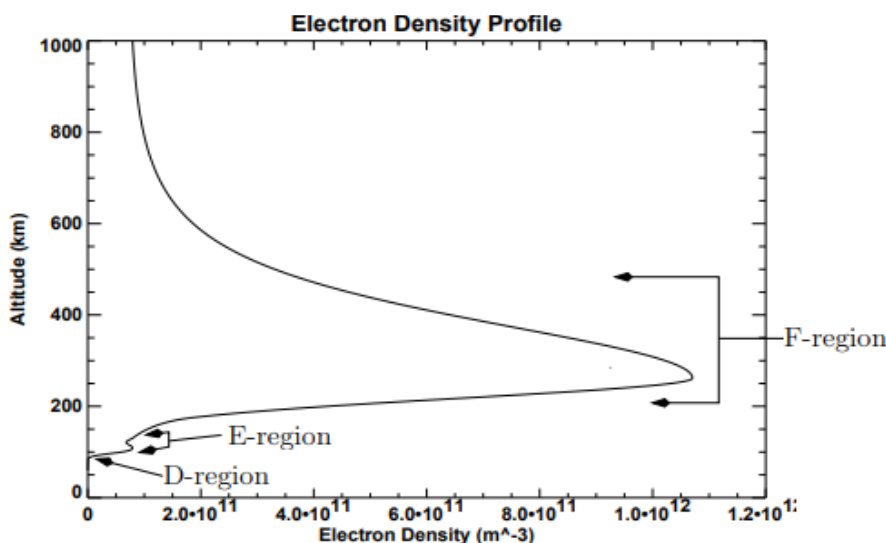


Figure 1: A generalized profile of electron density [8]

Over the last decades, many studies and researches related to the ionospheric HF propagation parameters were conducted, including the study of Aradhna S., et al. (2013), studied solar activity by studying the correlations between different solar parameters such as sunspot number, solar radio emission flux, coronal mass ejections, and solar X-ray background during January 2009 to December 2011, which represent the rising phase of solar cycle 24. They found that there is a good correlation between various studied parameters [9]. Bacharuddin F., et al. (2018), they used Genetic algorithm method to predicted allocation of Optimum Work Frequency OWF parameter to support long distance HF communication for marine monitoring from Jakarta to Tanjung Pinang. Two modes were used one as main frequency channel and one as reserve frequency channel (1F, 2E mode) for 24 hours with different antenna elevation. They found that the OWF frequency depends on the electron density in daytime or night and antenna elevation. The higher the electron density of the layer the higher the reflected frequency [10]. Hadi K. A., et al. (2020), studied the annual and seasonal reciprocal relationship between (MUF), (LUF) and (OWF) parameters during the annual and seasonal times of the years 2009 and 2014 over Iraqi zone. They suggested a fourth order polynomial equation to describe the seasonal and annual interrelationships between MUF and OWF parameters relative to LUF parameter, and a simple relationship (linear regression equation) to represent the relationship between the MUF and OWF [11].

The aim of this research is to investigate type of the annual cross-correlation between three different ionospheric parameters; these are *Optimum Working Frequency* OWF, *Highest Probable Frequency* HPF, and *Best Usable Frequency* BUF. The investigation intends to be conducted for Middle East Region during the minimum and maximum years of solar cycle 24 (SC 24), 2009 and 2014 respectively.

## 2. Ionosphere Communication Parameters

One of the most important solar activity parameters that can affects on the ionospheric communication process is the sunspot numbers (SSN), that fluctuates with a cyclical variation over around 11-years, which is also called "sunspot cycle or solar cycle" [12, 13]. The ionospheric communication parameters depends on the variations of the ionosphere layer which play as the main transport medium of High-Frequency (HF) radio waves propagation [14, 15]. Ionospheric parameters which described the optimal radio frequency values are widely used and recommended for ionospheric long-term studies and predictions [16]. There are several parameters which represent the key technologies of HF communication such as OWF, HPF, and BUF.

Working frequency needed to provide a successful HF radio contact between two points, must be lower than the MUF which represent the highest frequency at which radio waves are reflected back to Earth by ionosphere, this frequency (working frequency) called OWF, which can exceed roughly 85% of the MUF [10, 17, 18], while the frequency parameter that represent the highest frequency with the ionospheric conditions at which radio waves can be used to communicate across a specified path and at a given time that provide communication of 10% of the days, which represent about three days in a given month this parameter known as the HPF [19]. Whereas, the HF frequency signal that can be transmitted and received with most effectively for a given distance and specific time that has the highest signal-to-noise ratio (S/N) and the specified minimum take-off angle is referred by the BUF [20].

## 3. Geodesic Parameter Calculations

In order to establish HF radio communication link, it is necessary to have an information about the geodesic coordinates for the locations of the transmitter/receiver station. In this

work, the Middle East region was selected to be the study area, where Baghdad city (Lat. 33.35° N, Long. 44.42° E) was adopted as a transmitter station (T<sub>x</sub>) and other thirty-two stations that lies on different bearings (N, NE, E, SE, S, SW, W, NW) and path lengths (500, 1000, 1500, and 2000) km from the transmitter station was selected to be as receiving stations (R<sub>x</sub>). The geodesic coordinate parameters (geographical coordinate: latitude and longitude) of the selected receiver stations were calculated using equations (1) and (2)[21, 22]. The calculations were performed using a MatLab program that was designed and implemented for this purpose. Figure (2) illustrates the distribution of the calculated geographical coordinates for the determined receiving stations.



**Figure 2:** The distribution for the locations of the determined receiver stations coordinates (latitudes and longitudes) over the Middle East Region.

$$\varphi_2 = \text{asin}(\sin\varphi_1 \cos \delta + \cos \varphi_1 \sin \delta \cos \theta) \quad \dots \dots (1)$$

$$\lambda_2 = \lambda_1 + \text{atan2}(\sin \theta \sin \delta \cos \varphi_1, \cos \delta - \sin \varphi_1 \sin \varphi_2) \quad \dots \dots (2)$$

Where,  $\varphi$ : latitude,  $\lambda$ : longitude,  $\theta$ :the bearing (clockwise from north),  $\delta$ : the angular distance  $d/R$ ,  $d$ : path length,  $R$ : Earth’s radius (6,371 km)

**4. Test and Results**

The OWF, HPF and BUF ionospheric parameters are crucial for HF radio communication. In this research the type of the annual cross-correlation between the three tested parameters was investigated. The investigation was conducted during the minimum and maximum years of SC 24, 2009 and 2014 respectively. The monthly predicted dataset for the studied parameters was generated using VOCAP and ASAPS HF-international models. The parametric generation was performed for all selected geodetic parameters and the adopted time periods based on the monthly mean values of SSN. Table (1) presents the monthly mean SSN values for the minimum and maximum years of SC 24 (2009 and 2014), consecutively.

**Table 1:** Monthly mean Sunspot number for minimum and maximum years of SC-24 [23]

	Jan.	Feb.	Mar.	Apr.	May.	Jun.	Jul.	Aug.	Sep.	Oct.	Nov.	Dec.
<b>2009</b>	1.3	1.2	0.6	1.2	2.9	6.3	5.5	0.0	7.1	7.7	6.9	16.3
<b>2014</b>	117	146.1	128.7	112.5	112.5	102.9	100.2	106.9	130	90	103.6	112.9

The datasets of HPF, OWF parameters were generated using VOCAP model, while the BUF parameter values were generated using ASAPS model. The annual average variations of OWF, HPF, and BUF ionospheric parameters were computed for all geodesic parameters (path lengths and bearings) depending on the monthly predicted datasets. Figure 3 shows examples of the annual average variation patterns for OWF, HPF and BUF ionospheric parameters for path 1000 km and bearing =0, left for year 2009 and right for year 2014 from SC 24.

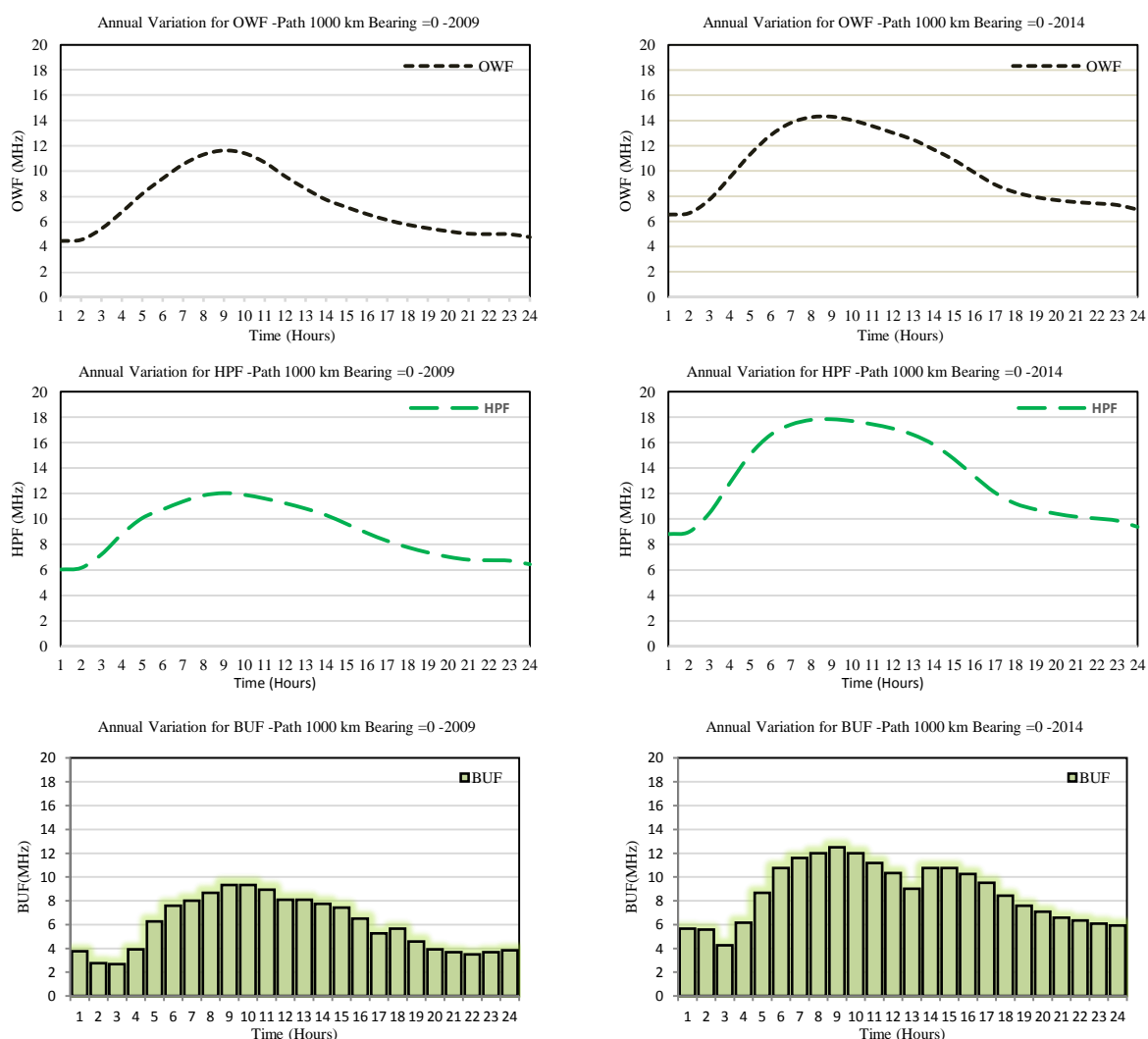


**Figure 3:** samples of annual behavior of smoothed OWF, HPF and fluctuated BUF ionospheric parameters for minimum and maximum years of SC(24), the left for year 2009 while the right for 2014

In Figure 3, the annual average predicted values of HPF and OWF parameters exhibited a smoothed behavior while the values of BUF parameter displayed fluctuating values, which agreed with the conventional measurements. To overcome these irregularities and establish a standardized annual pattern for all three parameters, mathematical smoothing techniques were

applied to the predicted BUF values. This process helped to produce unified behavior of the data and get a smooth underlying trend. Figure 4 shows samples of the smoothed behavior of the annual variation for the three studied ionospheric parameters HPF, OWF and BUF, with different path lengths and bearing for minimum and maximum years of SC 24.

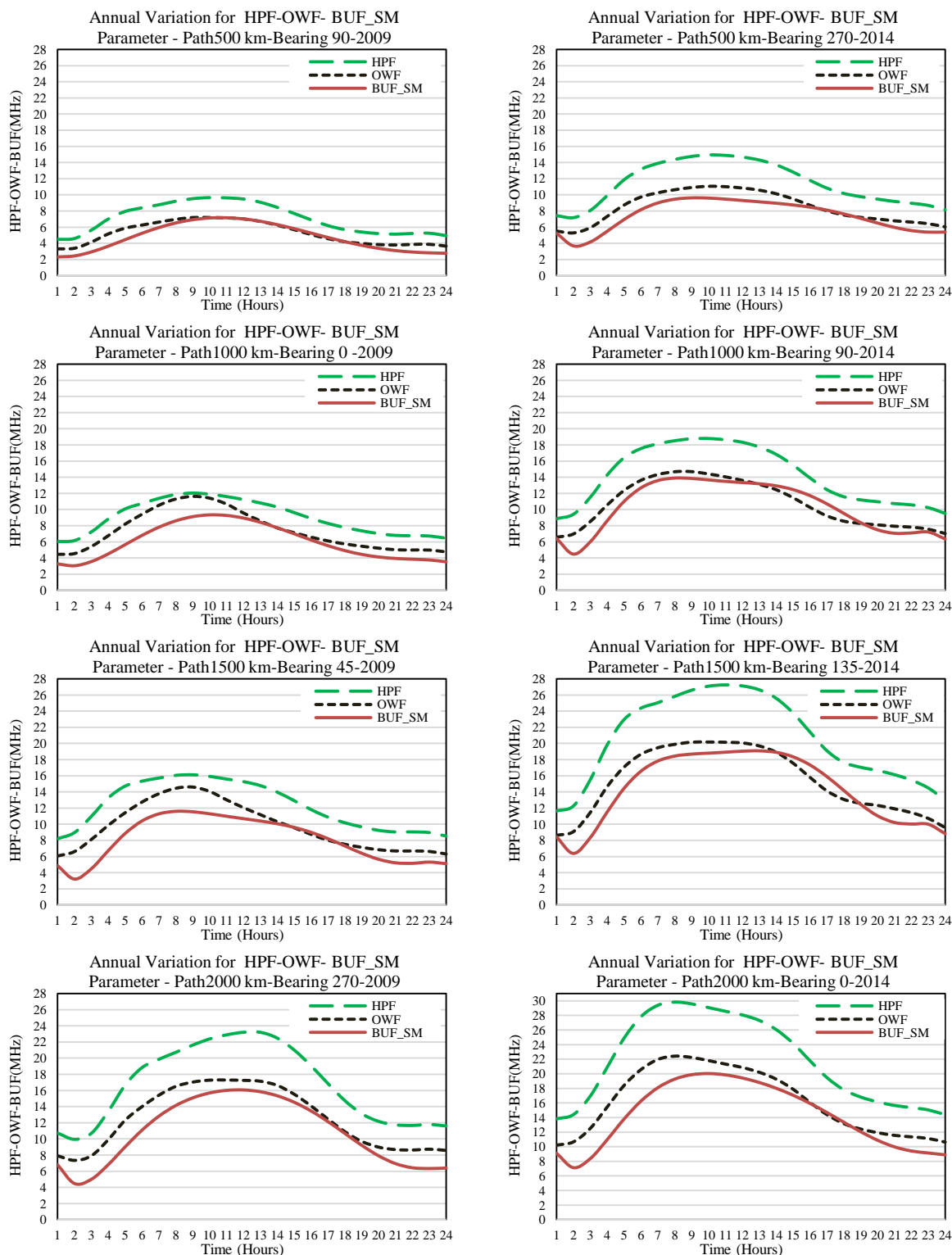


**Figure 4:** Samples of annual smoothed behavior of HPF, OWF and BUF ionospheric parameters of minimum and maximum years of SC 24 ,the left for year 2009 while the right for 2014 .

To investigate the type of the annual Cross-Correlation among the selected ionospheric parameters (HPF, OWF and BUF), various cross-correlation methods including exponential, linear, logarithmic, polynomial, and Power methods were applied. The cross-correlation tests were conducted for each pair of parameters, including [(OWF vs. BUF), (OWF vs. HPF), (HPF vs. OWF), (HPF vs. BUF), (BUF vs. OWF), and (BUF vs. HPF)]. The tests were performed for the two studied years and for all (32) selected locations based on the adopted geodesic parameters, path lengths (500, 1000, 1500, and 2000) km and bearings (N, NE, E, SE, S, SW, W, NW).

The type and order of the annual cross-correlation methods for the tested parameter pairs were investigated and elected depending on the highest determination coefficient values ( $R^2$ ), that give the best order which can describe the correlation method between the tested parameter pairs. Samples of the investigating results of the annual cross-correlation between the tested parameters during the selected studied years of solar cycle 24 were illustrated in Table (2) for year 2009 and Table (3) for year 2014

**Table 2:** Samples of Investigating results of the Annual correlation between the studied parameters for the year 2009 based on the determination coefficient ( $R^2$ ) values

<b>OWF(BUF)_ Path 500 km _SC 24_2009.</b>						
Bearing	Exp.	Linear	Log.	Polynomial		power
				2 <sup>nd</sup> order	3 <sup>rd</sup> Order	
NE	0.8965	0.9061	0.8912	0.9061	0.9062	0.8989
E	0.9094	0.9141	0.8918	0.9147	0.9148	0.9069
SE	0.9177	0.9108	0.8773	0.9152	0.9155	0.905
W	0.9292	0.9283	0.8949	0.9308	0.9308	0.9168
<b>BUF(OWF)_ Path 1000 km _SC 24_2009.</b>						
Bearing	Exp.	Linear	Log.	Polynomial		power
				2 <sup>nd</sup> order	3 <sup>rd</sup> Order	
N	0.8518	0.8789	0.8995	0.9009	0.9013	0.8947
S	0.7779	0.8353	0.8719	0.8826	0.8829	0.8321
SW	0.8045	0.8586	0.8958	0.9042	0.9060	0.8617
NW	0.8513	0.9083	0.9251	0.9251	0.9257	0.8907
<b>HPF(OWF)_ Path 1500 km _SC 24_2009.</b>						
Bearing	Exp.	Linear	Log.	Polynomial		power
				2 <sup>nd</sup> order	3 <sup>rd</sup> Order	
NE	0.9324	0.9587	0.9876	0.9978	0.9984	0.9745
E	0.9472	0.9653	0.9847	0.9893	0.9916	0.9809
SW	0.9708	0.9790	0.9728	0.9799	0.9799	0.9892
W	0.9486	0.9643	0.9790	0.9818	0.9844	0.9802
<b>BUF(HPF)_ Path 2000 km _SC 24_2009.</b>						
Bearing	Exp.	Linear	Log.	Polynomial		power
				2 <sup>nd</sup> order	3 <sup>rd</sup> Order	
NE	0.8370	0.8785	0.8691	0.8802	0.8819	0.8389
E	0.8375	0.9034	0.8973	0.9034	0.9034	0.8425
SW	0.8649	0.9248	0.9279	0.9295	0.9302	0.9032
NW	0.9330	0.9265	0.9067	0.9383	0.9429	0.9275

**Table 3:** Samples of Investigating results of the Annual correlation between the studied parameters for the year 2014 based on the determination coefficient ( $R^2$ ) values.

<b>OWF(BUF)_ Path 500 km _SC 24_2014.</b>						
<b>Bearing</b>	<b>Exp.</b>	<b>Linear</b>	<b>Log.</b>	<b>Polynomial</b>		<b>power</b>
				<b>2<sup>nd</sup> order</b>	<b>3<sup>rd</sup> Order</b>	
<b>N</b>	0.8987	0.9043	0.8827	0.9055	0.9149	0.8926
<b>E</b>	0.8737	0.8592	0.8203	0.8837	0.8875	0.8466
<b>SE</b>	0.8368	0.8154	0.7649	0.8402	0.8416	0.7988
<b>NW</b>	0.9181	0.9097	0.8519	0.9397	0.9397	0.8755
<b>BUF(OWF)_ Path 1000 km _SC 24_2014.</b>						
<b>Bearing</b>	<b>Exp.</b>	<b>Linear</b>	<b>Log.</b>	<b>Polynomial</b>		<b>power</b>
				<b>2<sup>nd</sup> order</b>	<b>3<sup>rd</sup> Order</b>	
<b>E</b>	0.8278	0.886	0.8988	0.9004	0.9004	0.8536
<b>S</b>	0.8877	0.9255	0.9280	0.9311	0.934	0.9143
<b>SW</b>	0.8967	0.9360	0.9403	0.9423	0.9436	0.9252
<b>NW</b>	0.8385	0.9002	0.9144	0.9132	0.9220	0.8689
<b>OWF(BUF)_ Path 1500 km _SC 24_2014.</b>						
<b>Bearing</b>	<b>Exp.</b>	<b>Linear</b>	<b>Log.</b>	<b>Polynomial</b>		<b>power</b>
				<b>2<sup>nd</sup> order</b>	<b>3<sup>rd</sup> Order</b>	
<b>N</b>	0.8802	0.8691	0.8061	0.9039	0.9039	0.8299
<b>S</b>	0.9270	0.9339	0.9087	0.9345	0.9347	0.9294
<b>SW</b>	0.9455	0.9528	0.9309	0.9530	0.9531	0.9503
<b>NW</b>	0.9123	0.8981	0.8532	0.9164	0.9164	0.8823
<b>HPF(BUF)_ Path 2000 km _SC 24_2014.</b>						
<b>Bearing</b>	<b>Exp.</b>	<b>Linear</b>	<b>Log.</b>	<b>Polynomial</b>		<b>power</b>
				<b>2<sup>nd</sup> order</b>	<b>3<sup>rd</sup> Order</b>	
<b>N</b>	0.8935	0.8918	0.8620	0.8965	0.9001	0.8763
<b>S</b>	0.8830	0.8800	0.8519	0.8905	0.8910	0.8651
<b>S</b>	0.9370	0.9536	0.9264	0.9537	0.9549	0.9456
<b>NW</b>	0.8924	0.8876	0.8671	0.8885	0.8912	0.8853

According to the investigation results of the annual cross-correlations for the predicted datasets of the three tested ionospheric parameters shown in Tables 2 and 3. The annual cross-correlation between (OWF-HPF) parameters showed a stronger correlation than the correlation between (OWF-BUF) and (HPF-BUF) parameter pairs on most path lengths and bearings during the maximum and minimum years of SC24.

Depending on the investigation results of the annual cross-correlation, annual correlative equations that can predict the ionospheric parameters values between each tested parameter pairs were derived. The derived equations were described as a polynomial mathematical equation. The results elucidate that the polynomial equation which can provided the best mathematical description of the better annual cross-correlation strength between the tested ionospheric parameters pairs is the third order polynomial equation. The proposed equations can be presented by the following set of equations:

$$\begin{aligned}
 HPF &= \sum_{i=0}^{\infty} C_i(OWF)^i \\
 OWF &= \sum_{i=0}^{\infty} C_i(HPF)^i \\
 HPF &= \sum_{i=0}^{\infty} C_i(BUF)^i && \dots \dots \dots (3) \\
 BUF &= \sum_{i=0}^{\infty} C_i(HPF)^i \\
 OWF &= \sum_{i=0}^{\infty} C_i(BUF)^i \\
 BUF &= \sum_{i=0}^{\infty} C_i(OWF)^i
 \end{aligned}$$

Where:  $C_i$  = correlation coefficient for the ( $i^{th}$ ) order of the polynomial equation.

Samples of the determined correlation coefficient sets ( $C_i$ ) for each correlation parameters pair that demonstrated in Eq. (3) were presented in Table (4) for year 2009 and Table (5) for year 2014.

**Table 4:** Samples of Correlation Coefficients of the cross-correlation equation of the minimum year of SC 24(2009)

		Path 500 km- Bearing SE -2009				Path 1000 km- Bearing S -2009			
		$C_0$	$C_1$	$C_2$	$C_3$	$C_0$	$C_1$	$C_2$	$C_3$
OWF	HPF	-0.0586	0.7503			8.712	-2.3885	0.3501	-0.0119
	BUF	1.4928	0.9558	-0.0883	0.0095	1.4423	1.4621	-0.2247	0.018
HPF	OWF	0.0824	1.332			3.927	-0.4902	0.2775	-0.014
	BUF	1.4422	1.7445	-0.2274	0.0206	0.0402	3.1453	-0.517	0.0346
BUF	OWF	-9.1578	5.4638	-0.7321	0.0393	-6.6837	3.1308	-0.1891	0.0035
	HPF	-9.275	4.1149	-0.4154	0.0168	-4.2109	1.4286	-0.0056	-0.0018
		Path 1500 km- Bearing SW -2009				Path 2000 km- Bearing E -2009			
		$C_0$	$C_1$	$C_2$	$C_3$	$C_0$	$C_1$	$C_2$	$C_3$
OWF	HPF	10.089	-1.869	0.2103	-0.0052	0.9591	0.5956	0.0052	
	BUF	5.5772	-0.29	0.0928	-0.0016	11.685	-1.6074	0.2113	-0.0056
HPF	OWF	-0.6274	1.5566	-0.0162		2.6899	0.5264	0.0824	-0.0027
	BUF	3.6969	1.3805	-0.1154	0.0071	15.231	-1.9697	0.2654	-0.0071
BUF	OWF	-11.936	4.1034	-0.2534	0.0062	-0.7486	0.3661	0.0763	-0.0024
	HPF	-9.3123	2.4079	-0.0938	0.0016	-3.3531	0.8479		

**Table 5:** Samples of Correlation Coefficients of the cross-correlation equation of the maximum year of SC 24 ( 2014)

		Path 500 km- Bearing N -2014				Path 1000 km- Bearing SW -2014					
		C <sub>0</sub>	C <sub>1</sub>	C <sub>2</sub>	C <sub>3</sub>			C <sub>0</sub>	C <sub>1</sub>	C <sub>2</sub>	C <sub>3</sub>
OWF	HPF	0.017	0.7375			OWF	HPF	7.0167	-0.8417	0.1129	-0.0025
	BUF	18.119	-7.1801	1.2569	-0.0614		BUF	1.3266	1.4899	-0.1058	0.0049
HPF	OWF	-0.0228	1.3558			HPF	OWF	3.6354	0.1322	0.1337	-0.0048
	BUF	25.05	-9.9782	1.7417	-0.0851		BUF	0.8182	2.3613	-0.1787	0.0076
BUF	OWF	-33.394	14.187	-1.7259	0.0722	BUF	OWF	3.8617	-0.9476	0.232	-0.0083
	HPF	-33.781	10.607	-0.9548	0.0295		HPF	6.2065	-1.1818	0.1571	-0.0039
		Path 1500 km– Bearing NW -2014				Path 2000 km- Bearing NE -2014					
		C <sub>0</sub>	C <sub>1</sub>	C <sub>2</sub>	C <sub>3</sub>			C <sub>0</sub>	C <sub>1</sub>	C <sub>2</sub>	C <sub>3</sub>
OWF	HPF	-15.032	3.6282	-0.1813	0.0037	OWF	HPF	-4.0844	1.359	-0.0305	0.0005
	BUF	8.7752	-0.2754	0.0501			BUF	18.307	-2.0359	0.17	-0.0029
HPF	OWF	10.71	-1.4353	0.2371	-0.0066	HPF	OWF	5.257	0.2765	0.0715	-0.0015
	BUF	15.371	-1.5258	0.1897	-0.0042		BUF	26.481	-3.1886	0.2653	-0.0049
BUF	OWF	-19.344	4.4902	-0.2047	0.0036	BUF	OWF	-29.153	6.1306	-0.3027	0.0056
	HPF	-31.602	5.6623	-0.2579	0.0044		HPF	-34.552	5.3464	-0.2052	0.0029

The proposed mathematical equations (Eq. (3)) were investigated by comparing their results of the annual HPF, OWF, and BUF parameter values with the predicted datasets generated using VOCAP and ASAPS models. The comparison was conducted for all adopted geodetic conditions and for the two adopted years (2009 and 2014) of SC 24. The comparison results were presented in Figure 5.

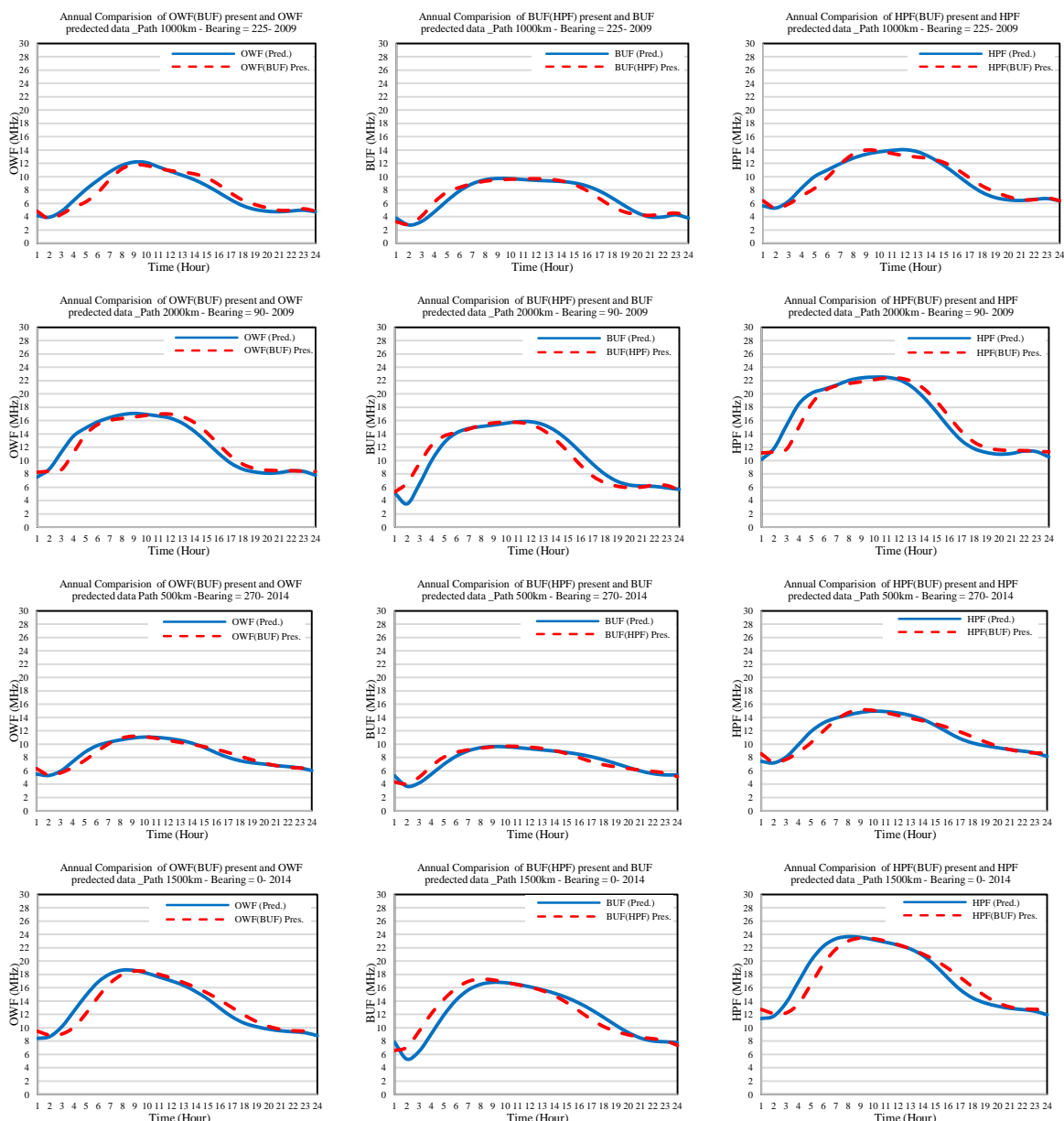


**Figure 5:** Samples of a comparison between the generated datasets using the proposed equations and the predicted values generated using VOCAP and ASAPS models for the annual times of the years 2009 and 2014.

For comparison, the behavior and distribution between the calculated (present and predicted) datasets of HPF, OWF and BUF ionospheric parameters were represented by contours plot diagrams. The comparison was performed for all geodesic parameters (path lengths and bearings) of the thirty-two receiving stations during the tested years (2009 & 2014). Figures 6 and 7 show contour plot diagrams for the present and predicted data for minimum and maximum years of SC 24 respectively. Form the Figures, the predicted and present annual average values of OWF,HPF, and BUF showed almost the same behavior and distribution (semi-circular shape) for all geodesic parameters that covering the studied area for minimum and maximum years of SC24 (2009 and 2014) respectively. Also these diagrams showed that the frequency values for all tested parameters were increased with increasing the distance between the transceiver stations, noting that this increment is more in the southern part of the studied area, and this may due to the influence of the thermal and geographical equators.

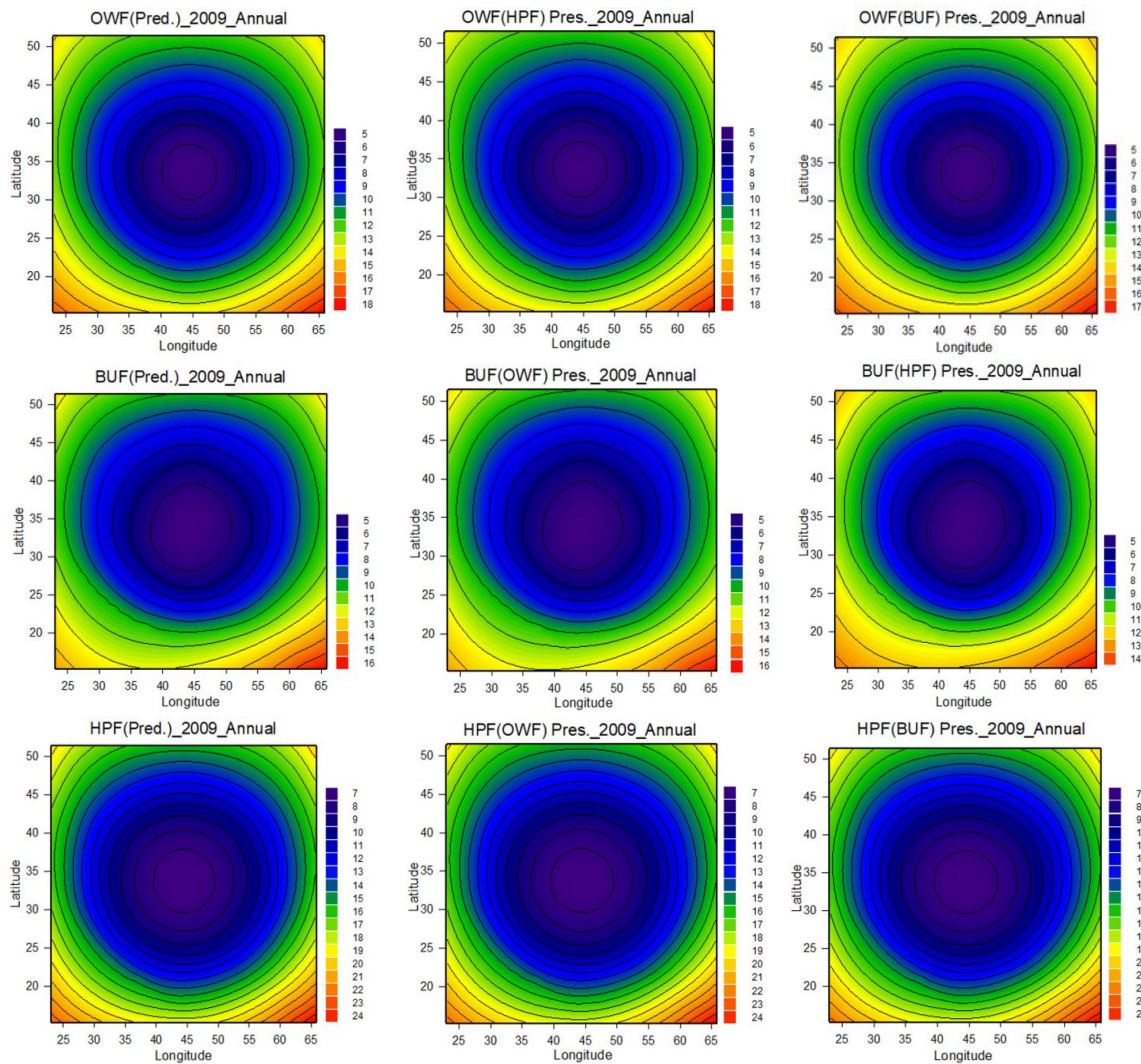


**Figure 6:** Contour plots for present and predicted ionospheric parameters for all geodesic studied parameter (path lengths and bearings) of the thirty-two receiving stations during 2009.

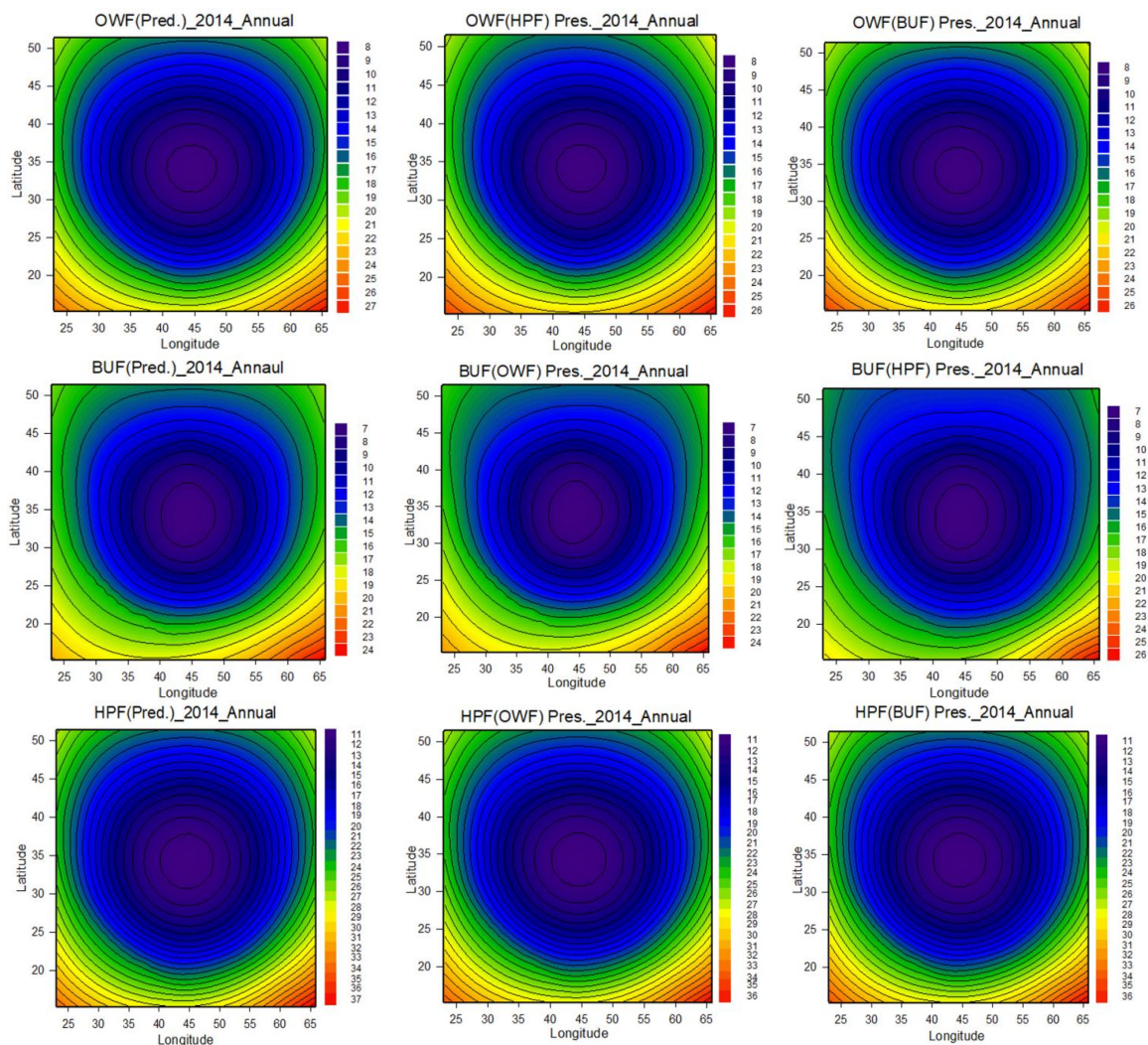


**Figure 7:** Contour plots for present and predicted ionospheric parameters for all geodesic studied parameter (path lengths and bearings) of the thirty-two receiving stations during 2014.

To assess the accuracy of the values calculated using the proposed cross-correlation equations relative to the predicted ionospheric parameter values generated using VOCAP and ASAPS international models, statistical calculation methods were applied using, Normalized Root Mean Square Error (NRMSE), Variance, Normalized Mean Absolute Error (NMAE) methods. Tables 6 and 7 illustrate samples of the statistical calculation results.

**Table 6:** Samples of the statistical calculations results for the annual variations of the minimum year (2009) of SC 24, for different Path length and Bearings

Path length: 500 km					Path length: 1000 km				
	Bearing	NRMSE	Variance	NMAE		Bearing	NRMSE	Variance	NMAE
OWF(BUF)	N	0.0731	0.1402	0.0580	HPF (BUF)	NE	0.0650	0.3456	0.0459
	E	0.0771	0.0604	0.1632		SE	0.0889	0.7125	0.0690
	S	0.0719	0.1488	0.0576		SW	0.0531	0.2612	0.0377
	W	0.0695	0.1345	0.0575		NW	0.0530	0.2322	0.0337
Path length: 1500 km					Path length: 2000 km				
	Bearing	NRMSE	Variance	NMAE		Bearing	NRMSE	Variance	NMAE
BUF(HPF)	N	0.0948	0.5530	0.0691	OWF (BUF)	N	0.0620	0.5186	0.0497
	NE	0.1217	0.9619	0.0832		E	0.0839	1.0523	0.0643
	W	0.0965	0.6900	0.0789		SE	0.1197	2.4481	0.0979
	NW	0.0717	0.3403	0.0583		W	0.0640	0.6402	0.0493

**Table 7:** Samples of the statistical calculations results for the annual variations of the maximum year (2014) of SC 24, for different Path length and Bearings

Path length: 500 km					Path length: 1000 km				
	Bearing	NRMSE	Variance	NMAE		Bearing	NRMSE	Variance	NMAE
HPF(OWF)	NE	0.0010	0.0001	0.0008	BUF (OWF)	N	0.0925	0.6485	0.0665
	SE	0.0014	0.0003	0.0011		E	0.0943	0.9275	0.0684
	SW	0.0602	0.2694	0.0455		SW	0.0675	0.5015	0.0541
	NW	0.0014	0.0003	0.0011		NW	0.0737	0.4740	0.0556
Path length: 1500 km					Path length: 2000 km				
	Bearing	NRMSE	Variance	NMAE		Bearing	NRMSE	Variance	NMAE
BUF(HPF)	E	0.0992	1.7804	0.0748	OWF (BUF)	N	0.0864	1.9359	0.0706
	S	0.0727	1.2058	0.0622		E	0.0877	2.4635	0.0640
	SW	0.0614	0.7460	0.0584		S	0.0589	1.5232	0.0501
	NW	0.0845	1.0793	0.0692		W	0.0579	1.1332	0.0445

### 5. Conclusions

Based on the results reached, the conclusions can be summarized by the following points:

- The values of the ionospheric parameters (HPF, OWF, and BUF) increase with increasing the path length between the transmitting and receiving stations.
- The values of the HPF parameter showed higher values than the values of the OWF and BUF parameters and this may be due to the fact that it represents the value of the highest communication frequency of the HF link rather than being the optimum frequency.
- Contour plots diagrams for the present and predicted annual datasets of the tested parameters showed almost the same behavior and distribution (semi-circular shape) for all adopted directions (Bearings) during the studying years. Also, the contour plot diagrams showed that the frequency values for all tested parameters were increased with the increment

of the distance value (path length) from the transmitting station, noting that this increment is more in the southern part of the studied area, and this may due to the influence of the thermal and geographical equators.

- The investigation results showed that the best mathematical equation which can provide a better description of the annual cross-correlation between the studied ionospheric parameters for all tested path lengths and bearings of the two adopted years is a third-order polynomial equation.
- Different statistical calculation results of the calculated datasets produced by the suggested mathematical equations for the three studied parameters of the annual variation of the two tested years showed good results for all path-lengths, and bearings.

## References

- [1] V. Barta, J. Chum, H.-L. Liu, D. Pokhotelov, and G. Stober, "Editorial for the Special Issue: Vertical Coupling in the Atmosphere-Ionosphere-Magnetosphere System," *Frontiers in Astronomy and Space Sciences*, vol. 10, 2024. <http://dx.doi.org/10.3389/fspas.2023.1359458>.
- [2] A. A. Temur and A. F. Ahmed, "The Plasma Characteristics of the Earth's Ionosphere in F-layer," *Iraqi Journal of Science*, vol. 63, no. 7, pp. 3225-3235, 2022. <http://dx.doi.org/10.24996/ijs.2022.63.7.41>.
- [3] M. K. Mardan and K. A. Hadi, "Study the Influence of Solar Activity on the Ionospheric Electron, Ion and Neutral Particle Temperatures over Iraqi Region Using Ionospheric Models," *Iraqi Journal of Science*, vol. 59, no. 1A, pp. 209 - 217, 2018. <http://dx.doi.org/10.24996/ijs.2018.59.1A.22>.
- [4] J. Male, J. Porte, T. Gonzalez, J. M. Maso, J. L. Pijoan, and D. J. S. Badia, "Analysis of the Ordinary and Extraordinary Ionospheric Modes for NVIS Digital Communications Channels," *Sensors*, vol. 21, no. 6, pp. 1-16, 2021. <https://doi.org/10.3390/s21062210>.
- [5] O. V. Mandrikova, N. V. Fetisova, Y. A. Polozov, I. S. Solovev, and M. S. Kupriyanov, "Method for modeling of the components of ionospheric parameter time variations and detection of anomalies in the ionosphere," *Earth, Planets and Space*, vol. 67, pp. 1-16, 2015. <http://dx.doi.org/10.1186/s40623-015-0301-4>.
- [6] M. Hervás, P. Bergadà, and R. M. Alsina-Pagès, "Ionospheric narrowband and wideband HF soundings for communications purposes: a review," *Sensors*, vol. 20, no. 9, pp. 1-27, 2020. <https://www.mdpi.com/1424-8220/20/9/2486#>.
- [7] L. Barclay, Ed. *Propagation of radiowaves, 2 nd edition* (IET Electromagnetic Waves Series 502). London, United Kingdom: The Institution of Engineering and Technology, 2003
- [8] R. G. Gillies, "Modelling of transionospheric HF radio wave propagation for the ISIS II and ePOP satellites," MSc., Physics and Engineering Physics, University of Saskatchewan Saskatoon, 2006. <https://www.researchgate.net/publication/255586549>
- [9] A. Sharma and S. R. Verma, "Solar Activity during the Rising Phase of Solar Cycle 24," *International Journal of Astronomy*, vol. 2013, pp. 212-216, 2013. <http://dx.doi.org/10.4236/ijaa.2013.33025>.
- [10] F. Bacharuddin, H. Wuryanto, Y. Yuliza, and B. Nugraha, "Optimum work frequency for marine monitoring based on genetic algorithm," *TELKOMNIKA*, vol. 16, no. 4, pp. 1551-1559, 2018. <http://dx.doi.org/10.12928/TELKOMNIKA.v16i4.7328>.
- [11] K. A. Hadi and M. D. Abdulkareem, "The Suggested Reciprocal Relationship between Maximum, Minimum and Optimum Usable Frequency Parameters Over Iraqi Zone," *Baghdad Science Journal*, vol. 17, no. 3, pp. 1058-1070, 2020. [http://dx.doi.org/10.21123/bsj.2020.17.3\(Suppl.\).1058](http://dx.doi.org/10.21123/bsj.2020.17.3(Suppl.).1058).
- [12] NASA Space Place. (2021). *Sunspots and Solar Flares*. Available: <https://spaceplace.nasa.gov/solar-activity/en/>
- [13] R. A. Malik, M. Abdullah, S. Abdullah, and M. J. Homam, "The influence of sunspot number on high frequency radio propagation," in *2014 IEEE Asia-Pacific Conference on Applied Electromagnetics (APACE)*, 2014, pp. 107-110: IEEE

- [14] D. A. Al-Shakarchi and M. I. Abd-almajied, "Response of The Ionospheric E-Region Critical Frequency and Virtual Height to the Solar Cycle 22 over Baghdad," *Iraqi Journal of Science*, vol. 63, no. 10, pp. 4576-4586, 2022. <http://dx.doi.org/10.24996/ijs.2022.63.10.39>.
- [15] R. Athieno and P. T. Jayachandran, "MUF variability in the Arctic region: A statistical comparison with the ITU-R variability factors," *Radio science*, vol. 51, no. 8, 2016.
- [16] M. Ahmad, I. Rashid, and N. Ahmad, "Validation of MUF and FOT parameters for plain, mountainous and sea region," in *International Conference on Information and Communication Technologies (ICICT)*, 2015, pp. 1-6: IEEE. <https://doi.10.1109/ICICT.2015.7469591>
- [17] A. K. Hasan, "Comparison of Prediction Programs for Short Wave Circuit Link from Iraq to Test points on Both Earth Hemispheres during Solar Minimum," *Al-Khwarizmi Engineering Journal*, vol. 17, no. 4, pp. 1-11, 2021. <https://doi.org/10.22153/kej.2021.10.003>.
- [18] M. Pietrella and M. Pezzopane, "Maximum usable frequency and skip distance maps over Italy," *Advances in Space Research*, vol. 66, no. 2, pp. 243-258, 2020. <https://doi.org/10.1016/j.asr.2020.03.040>.
- [19] The Official VOACAP Blog Updated. (2018). *Getting the best operating frequency from VOACAP P2P predictions*. Available: <https://voacap.blogspot.com/search?q=HPF>
- [20] S. A. Thabit, K. A. Hadi, and L. E. George, "Determination of the Annual Optimal Reliable Frequency for Different Transmitter/Receiver Stations Distributed over the Iraqi Territory," *Iraqi Journal of Science*, vol. 62, no. 4, pp. 1386-1395, 2021. <https://doi.org/10.24996/ijs.2021.62.4.34>.
- [21] Movable Type Scripts. *Calculate distance, bearing and more between Latitude\_Longitude points*. Available: <http://www.movable-type.co.uk/scripts/latlong.html>
- [22] wikipedia encyclopedia. *Great-circle distance*. Available: [https://en.wikipedia.org/wiki/Great-circle\\_distance](https://en.wikipedia.org/wiki/Great-circle_distance)
- [23] Solar Influences Data Analysis Center, Royal Observatory of Belgium *Sunspot Number, Sunspot Index and Long-term Solar Observations (SILSO)* Available: <https://www.sidc.be/SILSO/datafiles>